ChemPubSoc Europe

DOI: 10.1002/chem.201303868

CHEMISTRY A European Journal Full Paper

Dyes

meso-Ester and Carboxylic Acid Substituted BODIPYs with Far-Red and Near-Infrared Emission for Bioimaging Applications

Yong Ni,[a, b] Lintao Zeng,[c] Nam-Young Kang,[d] Kuo-Wei Huang,[e] Liang Wang,[c] Zebing Zeng,[a] Young-Tae Chang,*[a, d] and Jishan Wu*[a, b, f]

Abstract: A series of *meso*-ester-substituted BODIPY derivatives **1–6** are synthesized and characterized. In particular, dyes functionalized with oligo(ethylene glycol) ether styryl or naphthalene vinylene groups at the α positions of the BODIPY core (**3**–**6**) become partially soluble in water, and their absorptions and emissions are located in the far-red or near-infrared region. Three synthetic approaches are attempted to access the *meso*-carboxylic acid (COOH)-substituted BODIPYs **7** and **8** from the *meso*-ester-substituted BODIPYs. Two feasible synthetic routes are developed successfully, including one short route with only three steps. The *meso*-COOH-substituted BODIPY **7** is completely soluble in pure water, and its fluorescence maximum reaches around 650 nm with a fluorescence quantum yield of up to 15%. Time-dependent density functional theory calculations are conducted to understand the structure–optical properties relationship, and it is revealed that the Stokes shift is dependent mainly on the geometric change from the ground state to the first excited singlet state. Furthermore, cell staining tests demonstrate that the *meso*-ester-substituted BODIPYs (**1** and **3**–**6**) and one of the *meso*-COOH-substituted BODIPYs (**8**) are very membrane-permeable. These features make these *meso*-ester- and *meso*-COOH-substituted BODIPY dyes attractive for bioimaging and biolabeling applications in living cells.

Introduction

The remarkable technological advances in the areas of bioimaging and sensing have created a demand for biocompatible fluorescent probes with excitation and emission in the far-red and near-infrared (NIR) region (650–900 nm), because they avoid the use of light, which may cause phototoxicity and an autofluorescent background.[1] Although numerous synthetic far-red and NIR fluorophores with exceptional brightness exist, some of them tend to be water-insoluble and membrane-impermeable owing to their hydrophobic character,[2] others show poor photostability and undesired aggregation (such as cyanine, squaraine derivatives),[3] and others exhibit unspecific binding to cellular components because of a lack of appropriate binding sites.[4]

4,4-Difluoro-4-borata-3a,4a-diaza-*s*-indacene, abbreviated as BODIPY, is a well-known fluorophore that is attracting increasing attention in various bioapplications because of its outstanding photophysical properties such as its excellent environmental stability, large molar absorption coefficients, and sharp fluorescence spectrum with high fluorescence quantum yield.[1b–d] For example, pH-activated fluorescence probes including a BODIPY dye have been developed recently for the detection of cancers and real-time therapy monitoring.[5] Moreover, new probes generated by combining a BODIPY-based pH-sensing unit with a bisphosphonate compound have been used for the selective detection of bone-resorbing osteoclasts in vivo.[6] However, the undesirable optical property of most BODIPY dyes, with absorption and emission located below 600 nm, is still one of the severe limitations for their bioimaging applications. In the past few decades, a large number of far-red and NIR BODIPYs have been synthesized through various chemical modification methods (Figure 1): 1) functionalization at the α, β, and *meso* sites of the BODIPY core to extend π conjugation and generate a push–pull structure;[7] 2) em-

[a] *Y. Ni, Z. Zeng, Prof. Y.-T. Chang, Prof. J. Wu*
Department of Chemistry, National University of Singapore
3 Science Drive 3, Singapore 117543 (Singapore)
Fax: (+65) 6779-1691
E-mail: chmcyt@nus.edu.sg
chmwuj@nus.edu.sg

[b] *Y. Ni, Prof. J. Wu*
NUS Environmental Research Institute, National University of Singapore
5A Engineering Drive 1, 02-01, Singapore 117411 (Singapore)

[c] *Prof. L. Zeng, Prof. L. Wang*
School of Chemical and Chemical Engineering
Tianjin University of Technology
Tianjin 300384 (China)

[d] *Dr. N.-Y. Kang, Prof. Y.-T. Chang*
Laboratory of Bioimaging Probe Development
*Singapore Bioimaging Consortium, A*STAR*

[e] *Prof. K.-W. Huang*
King Abdullah University of Science and Technology (KAUST)
Division of Physical Sciences and Engineering and
KAUST Catalysis Center
Thuwal 23955-6900 (Saudi Arabia)

[f] *Prof. J. Wu*
*Institute of Materials Research and Engineering, A*STAR*
3 Research Link, Singapore 117602 (Singapore)

Supporting information for this article is available on the WWW under http://dx.doi.org/10.1002/chem.201303868.

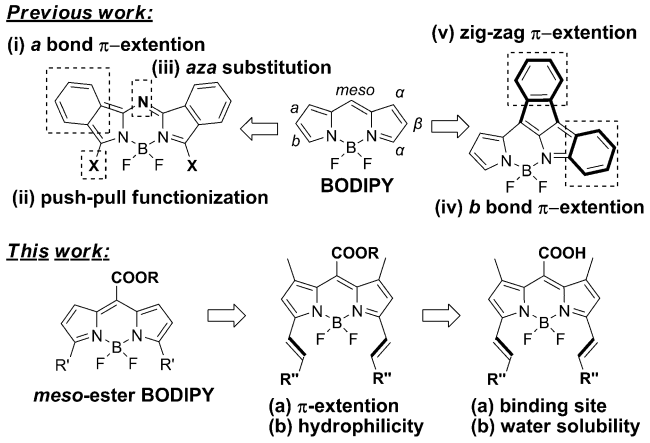

Figure 1. Previous and current strategies toward functional BODIPYs with long-wavelength absorption and emission.

ployment of π-extended pyrrole units instead of simple pyrrole to extend the conjugation configuration at the *a* or *b* bond of BODIPY;[8] 3) replacement of the *meso*-carbon with an imide-type nitrogen atom;[9] and 4) oxidative fusion of aromatic units at the zigzag edge to extend the π conjugation significantly.[10] Unfortunately, most of the generated BODIPYs showed low fluorescence quantum yields with small Stokes shifts, and tended to be too hydrophobic and membrane-impermeable. Moreover, the introduction of binding sites (such as carboxylic acid), which are essential for connection with some specific bioprobes to these π-extended BODIPY systems, was also a big synthetic challenge.

Herein, we propose a new design concept involving the introduction of an ester group to the *meso* position of the BODIPY (Figure 1) on the basis of the following considerations: 1) the ester group is an electron-withdrawing group, and it is easy to generate a push–pull-type structure and extend the π conjugation through functionalization at the α position of the BODIPY core, so it is possible to push the absorption and emission wavelengths to the far-red or NIR regions; 2) the ester group can be hydrolyzed to form a carboxylic acid group, which is an important binding site for various biomolecules and biocomponents,[11] and also a versatile functional group for further conjugation; 3) hydrophilic groups such as oligo(ethylene glycol) ether can be introduced easily through a condensation reaction at the α positions of the BODIPY to ensure the compounds are sufficiently hydrophilic and have good membrane permeability.[12] To the best of our knowledge, such BODIPY dyes have never been reported, although there are some BODIPYs with an ester or carboxylic group linked by an alkyl or phenyl spacer.[13,16] In this work, a series of *meso*-ester-substituted BODIPY dyes (**1**–**6**) and two *meso*-carboxylic-acid-functionalized BODIPY dyes (**7**, **8**) were prepared successfully (Figure 2). These new dyes exhibit tunable absorption and emission spectra in the far-red or even the NIR region, with acceptable fluorescence quantum yields and large Stokes shifts. Most of them have the appropriate hydrophilicity and are membrane-permeable. The successful conversion of the ester group to a carboxylic group provides many opportunities for further conjugation and specific binding studies. Our work started from the synthesis of the simplest *meso*-ester BODIPY **1**, moving to the more highly π-conjugated dye **2**, then to the push–pull-type dyes **3**–**6** with oligo(ethylene glycol) ether groups, and finally to the *meso*-COOH-substituted BODIPY dyes **7** and **8**, with the aim of tuning their absorption/emission wavelengths, fluorescence quantum yields, Stokes shifts, and hydrophilicities, and of introducing specific binding sites. Time-dependent density functional theory (TD DFT) calculations were conducted to gain more insight into their optical properties. Finally, cell-staining experiments were performed to probe their potentials for bioimaging and biolabeling applications.

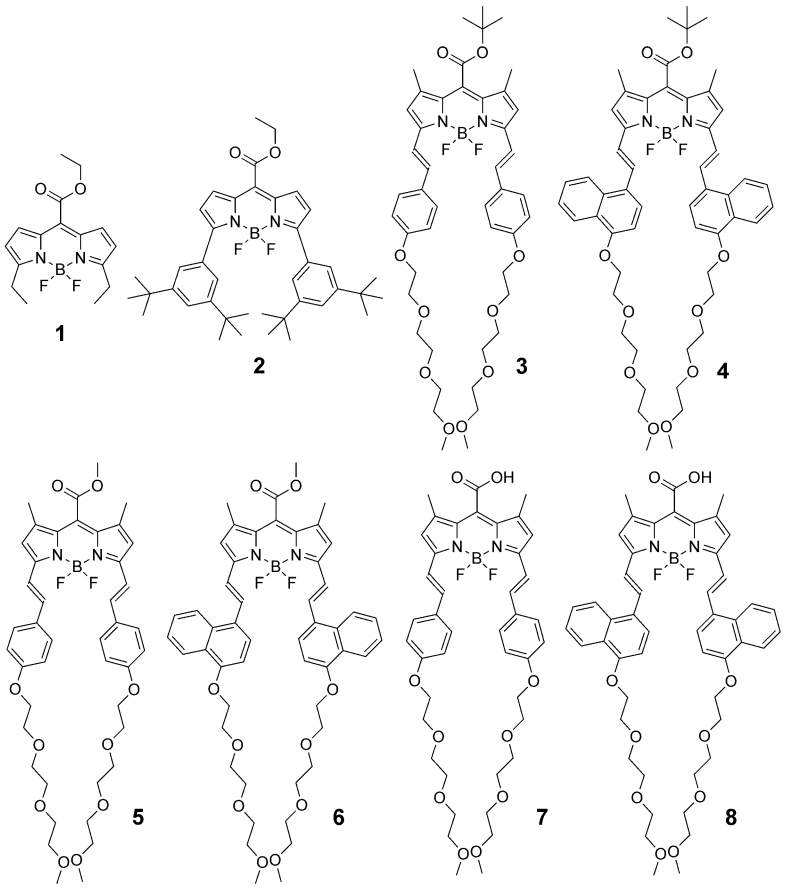

Figure 2. Chemical structures of the *meso*-ester- and COOH-substituted BODIPYs reported in this work.

Results and Discussion

Synthesis

The *meso*-ester-substituted BODIPYs **1** and **2** were prepared in 20% and 28% yield, respectively, through the condensation of ethyl glyoxalate (**9**) with 2-ethyl pyrrole (**10**) or 2-(3,5-di-*tert*-butylphenyl)pyrrole (**11**)[10a] in the presence of trifluoroacetic acid (TFA) in dichloromethane (DCM), followed by oxidative dehydrogenation with 2,3-dichloro-5,6-dicyano-1,4-benzoquinone (DDQ) and complexation with $BF_3{\cdot}Et_2O$ (Scheme 1).[14] Attempted hydrolysis of the ester groups in **1** and **2** with strong bases (e.g., KOH, NaOH, and LiOH) in highly polar solvents (THF, MeOH, and water) at room temperature all resulted in the decomposition of the starting materials, presumably because of nucleophilic attack on the B–F bonds (see Supporting Information).[15] Further modification and functionalization of these two molecules was difficult. Thus, a slight structural change was made by replacing the 2-ethyl pyrrole with 2,4-dimethylpyrrole; then, functionalization was possible through condensation with the corresponding aldehyde at the 3,5-methyl sites of the resulting BODIPYs. On the other hand, in an attempt to access *meso*-COOH-substituted BODIPYs, the hydrolysis reaction was performed on the benzyl (Bn)-*tert*-butyl- and methyl-protected ester groups, which will be discussed below (Scheme 1).

Palladium-catalyzed reduction was a preferable approach for achieving a carboxylic acid group from the benzyl ester, because it is a tidy reaction with a very high yield,[16] so benzyl-ester-substituted BODIPY was the first choice. Benzyl-2-chloro-2-oxoacetate **14** was obtained by adding one equivalent of benzyl alcohol (**12**) dropwise to the solution of oxalyl chloride (**13**) in dry chloroform.[17] The solution was then stirred at RT for 2 h, and the resulting compound **14** was used directly for the subsequent condensation reaction with 2,4-dimethylpyrrole at −78 °C, without further purification. After complexation with $BF_3{\cdot}OEt_2$, compound **15** was separated in a total yield of 45%. A low temperature was necessary for this condensation reaction, because the high reactivity of benzyl-2-chloro-2-oxoacetate generated many byproducts at RT, resulting in a much lower overall yield of 13%. The sufficient reactivity of the 3,5-methyl groups in **15** made functionalization at these positions realistic. Condensation of **15** with 4-(diphenylamino)benzaldehyde **16** gave the π-extended BODIPY **17** in 47% yield.[18] Hydrogenation of **17** was catalyzed by 10% Pd/C in a H_2 atmosphere (1 atm),[16] and thin-layer chromatography (TLC) analysis confirmed that the benzyl group was removed. However, the UV/Vis absorption spectrum and MALDI-TOF analysis of the product demonstrated that the double bonds linked to the 3,5-positions of BODIPY were also hydrogenated at the same time and gave the major product **18** (Supporting Information). Alternatively, the benzyl group in **15** was removed through a similar hydrogenation to give the *meso*-COOH-substituted BODIPY **19** in nearly quantitative yield. However, the subsequent condensation of compound **19** with 4-(diphenylamino) benzaldehyde did not occur under similar condensation conditions.

The *tert*-butyl ester group was hydrolyzed quite easily under acid conditions, so *meso-tert*-butyl-ester-substituted BODIPY could serve as another choice. The condensation reaction between *tert*-butyl-2-chloro-2-oxoacetate and 2,4-dimethylpyrrole at a low temperature (−78 °C) followed by oxidation and complexation produced the *meso-tert*-butyl-ester-substituted BODIPY **20** in very low yield (< 5%), because the *tert*-butyl

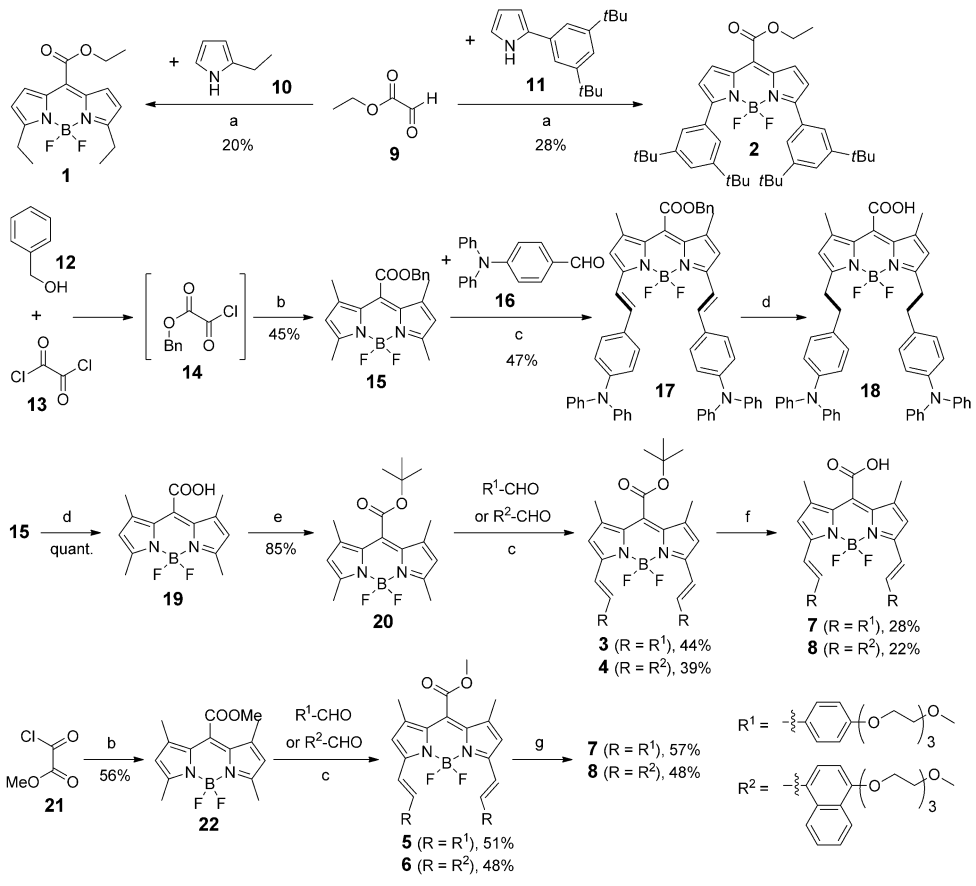

Scheme 1. Synthesis of the *meso*-ester and carboxylic-acid-functionalized BODIPYs **1**–**8**: a) i) $BF_3{\cdot}Et_2O$, CH_2Cl_2, RT, 3 h; ii) DDQ, RT, 1 h; iii) Et_3N, $BF_3{\cdot}Et_2O$, RT, 1 h; b) i) 2,4-dimethylpyrrole, −78 °C, 4 h; ii) Et_3N, $BF_3{\cdot}Et_2O$, $BF_3{\cdot}OEt_2$, −78 °C to RT, 2 h; c) piperidine, AcOH, toluene, reflux, 12 h; d) 10% Pd/C, 1 atm H_2, RT, 4 h; e) *tert*-butanol, DCC, anhydrous diethyl ether, RT, 5 h; f) HCl, CH_3NO_2, 0 °C to RT, 4 h; g) LiI, ethyl acetate, reflux, 8 h.

group was removed easily under acidic conditions. On the other hand, esterification of **19** in an excess of *tert*-butanol using *N*,*N*′-dicyclohexylcarbodiimide (DCC) as the dehydrating reagent gave **20** in 85% yield. Subsequent condensation with the corresponding oligo(ethylene glycol)-ether-substituted benzaldehyde and naphthalene aldehyde afforded the *meso*-*tert*-butyl ester BODIPYs **3** and **4** in 44% and 39% yields, respectively. Finally, hydrolysis of **3** and **4** with HCl (aq) in nitromethane at room temperature[19] gave the *meso*-COOH BODIPYs **7** and **8** in 28% and 22% separation yields, respectively. The TLC analysis showed that some of the starting material was decomposed; moreover, the high polarity of the carboxylic acid led to a significant loss of the compound during column chromatography on a silica gel column, resulting in a low separation yield. The generated *meso*-COOH-substituted BODIPYs **7** and **8** were fully soluble in pure water thanks to the carboxylic acid group at the *meso* site and the oligo(ethylene glycol) ether group localized at the other terminals.

The six-step synthetic approach toward the *meso*-COOH-substituted BODIPYs **7** and **8** was tedious and the overall yield was low. To simplify the synthesis, we finally developed a more convenient approach with fewer steps and a much higher overall yield. The *meso*-methyl-ester-substituted BODIPY **22** was synthesized from methyl chloro-oxalate (**21**) in 56% yield by using a similar procedure to that for **15** (Scheme 1). A similar condensation reaction of **22** with the corresponding aldehyde gave the *meso*-methyl-ester-substituted BODIPYs **5** and **6** in 51% and 48% yield, respectively. The hydrolysis of the *meso*-COOMe group again turned out to be the major challenge. We tried various conditions, but the use of a strong base resulted in decomposition, and with a strong acid such as HCl or an organic base such as triethylamine or pyridine, the methyl group could not be removed.[20] Fortunately, after many optimizations (see Supporting Information for details), we found that the use of the Lewis acid lithium iodide as reagent and ethyl acetate as solvent under reflux were the best conditions, providing the desired *meso*-COOH-substituted BODIPYs **7** and **8** in 57% and 48% yields, respectively.[21] The TLC analysis indicated that the conversion yield was nearly quantitative but the separation yield was much lower owing to the loss during purification. This approach has made the water-soluble *meso*-COOH-substituted BODIPYs **7** and **8** accessible in only three steps, and the separation yield of each step is around 50%. The structures of all these compounds were indentified unambiguously through NMR spectroscopy and mass spectrometry (Supporting Information).

Optical properties

The absorption and normalized emission spectra of **1** and **2** in DCM are shown in Figure 3 and the data are collected in Table 1. For dye **1**, the maximum absorption wavelength (λ_{abs}^{max}) is located at 536 nm, which is a bathochromic shift of 40 nm compared to those of the congeners with alkyl substituents.[4] The moderate bathochromic shift can be attributed to the inductive effect from the COOEt group, which is consistent with the results on the *meso*-CF_3-substituted BODIPY derivative

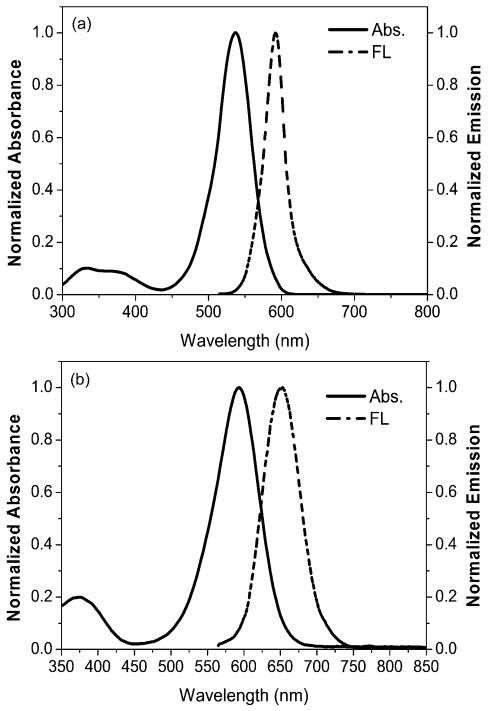

Figure 3. Normalized absorption (solid line), and emission (dashed line) spectra of a) dye **1** (λ_{ex} = 510 nm) and b) dye **2** (λ_{ex} = 560 nm) in CH_2Cl_2.

Table 1. Summary of optical data of dyes **1**–**8**.

Dye	Solvent	λ_{abs}^{max} [nm]	log ε [$M^{-1}cm^{-1}$]	λ_{em}^{max} [nm]	$\Delta\nu$ [cm^{-1}]	Φ
1	CH_2Cl_2	536	4.70	592	1765	0.78
2	CH_2Cl_2	592	4.40	653	1578	0.17
3	MeOH	657	4.80	684	601	0.19
4	MeOH	680	4.89	729	998	0.11
5	MeOH	658	5.08	663	115	0.06
6	MeOH	682	4.83	727	908	0.06
7	MeOH	627	4.48	642	373	0.36
	H_2O	628	4.36	646	544	0.15
8	MeOH	645	4.78	676	711	0.15
	H_2O	641	4.38	680	895	0.03

(λ_{abs}^{max} = 548 nm).[22] The maximum emission wavelength (λ_{em}^{max}) is at 592 nm, which is much longer than that of *meso*-CF_3-substituted BODIPY. The absorption and emission spectra of **1** are almost completely separate from each other with a large Stokes shift ($\Delta\nu$ = 1765 cm^{-1}). The unusually redshifted emission and large Stokes shift are probably associated with the remarkable geometrical difference between the first singlet excited state and the ground state (discussed in the DFT calculation section, vide infra).[23] In addition, **1** shows high fluorescence quantum yields (Φ = 0.63 in methanol and 0.78 in DCM) with good storage and photostability. The absorption spectrum of **2** is centered at 592 nm, whereas the emission maximum is located at 653 nm, also with a large Stokes shift ($\Delta\nu$ = 1578 cm^{-1}). In comparison with **1**, the aryl group at the 3,5-positions of BODIPY cause a notable bathochromic shift (60 nm) caused by the extended π conjugation. The fluorescence quan-

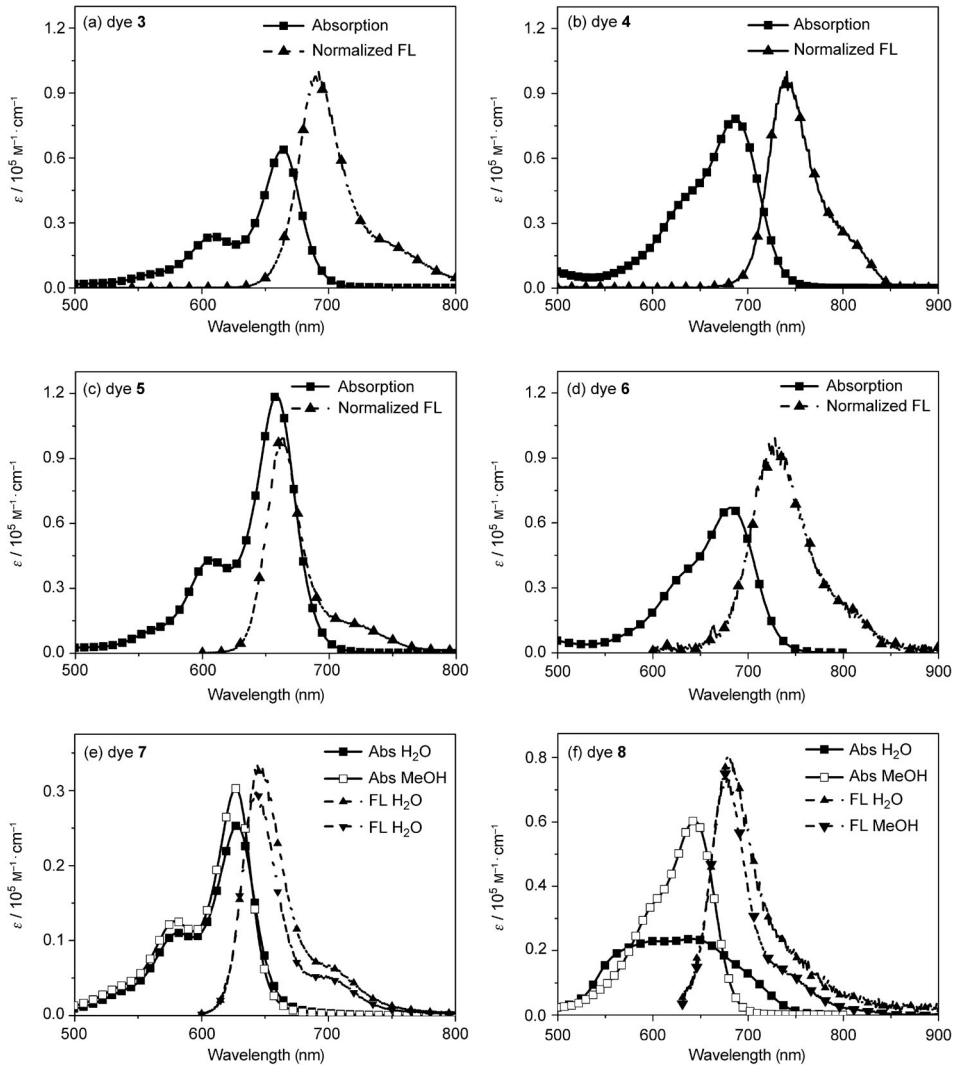

Figure 4. a–d) absorption (solid line) and normalized emission (dashed line) spectra of dyes **3**–**6** in methanol; e,f) absorption (solid line) and normalized emission (dashed line) spectra of dye **7** and **8** in methanol and pure water.

tum yield of **2** in DCM ($\Phi = 0.17$) is much lower than that of **1**, which can be attributed to nonirradiative energy loss arising from the free rotation of the aryl substituents.

After functionalization at the 3,5-positions by oligo(ethylene glycol)-ether-substituted styryl or naphthalene vinylene groups, the absorption and emission wavelength of dyes **3**–**6** in methanol displayed remarkable bathochromic shifts (Figure 4 and Table 1). The maximum absorption wavelength reaches approximately 658 nm for **3** and **5**, with fluorescence at 684 nm ($\Phi = 19\%$) and 663 nm ($\Phi = 6\%$), respectively. Dye **3** displays a larger Stokes shift ($\Delta\nu = 601\ cm^{-1}$) than **5** ($\Delta\nu = 115\ cm^{-1}$), but both are significantly smaller than those of **1** and **2**. Attachment of naphthalene groups at the 3,5-methyl position results in an even more significant bathochromic shift, with the absorption maxima of **4** and **6** at approximately 680 nm and fluorescence at around 728 nm ($\Phi = 11\%$ for **4** and $\Phi = 6\%$ for **6**). Large Stokes shifts of 998 cm^{-1} for **4** and 908 cm^{-1} for **6** were observed, which are desirable for NIR fluorophores. These four dyes show good solubility in highly polar solvents such as MeOH, DMSO, and even in PBS buffer solution containing 2% DMSO. Meanwhile, the storage and photostability of these BODIPY dyes are excellent. Notably, the fluorescence goes to the far-red and NIR region (above 700 nm) with an acceptable quantum yield and large Stokes shift. All these excellent features make these dyes very attractive for bioimaging applications.

After hydrolysis, the *meso*-COOH-substituted BODIPYs **7** and **8** were soluble in both methanol and water, and a blue-shift of their absorption and emission spectra was observed compared with their corresponding *meso*-ester analogs **3**–**6** (Figure 4 and Table 1). The λ_{abs}^{max} value of **7** centered at 627 nm in MeOH and 628 nm in pure water, whereas λ_{em}^{max} was located at 642 nm in methanol and 646 nm in pure water, with a remarkable fluorescence quantum yield ($\Phi = 36\%$ in methanol and $\Phi = 15\%$ in pure water). This can be regarded as a significant improvement for BODIPY dyes, especially for fluorophores with emission around or above 650 nm. For **8**, λ_{abs}^{max} goes to 645 nm in methanol and 641 nm in pure water, with λ_{em}^{max} located at 676 nm ($\Phi = 15\%$) and 680 nm ($\Phi = 3\%$), respectively. The prominent features of these two *meso*-COOH-substituted BODIPY dyes, namely, good water solubility, long wavelength absorption and emission, appreciable fluorescence quantum yields in pure water, the presence of carboxylic acid as a bonding site, and excellent storage and photostability, make them highly attractive for bioapplications.

DFT calculations

To gain more insight into the optical properties of these new *meso*-ester- and carboxylic-acid-substituted BODIPY dyes, we performed time-dependent (TD) DFT calculations at the B3LYP/6-31G*level of theory for the model compounds, as implemented in the Gaussian 09 program package.[24] The geometry optimizations for the first excited states of compounds **1** and **5** (root = 1) were conducted using the default SCRF method with the integral equation formalism variant (IEFPCM) in dichloro-

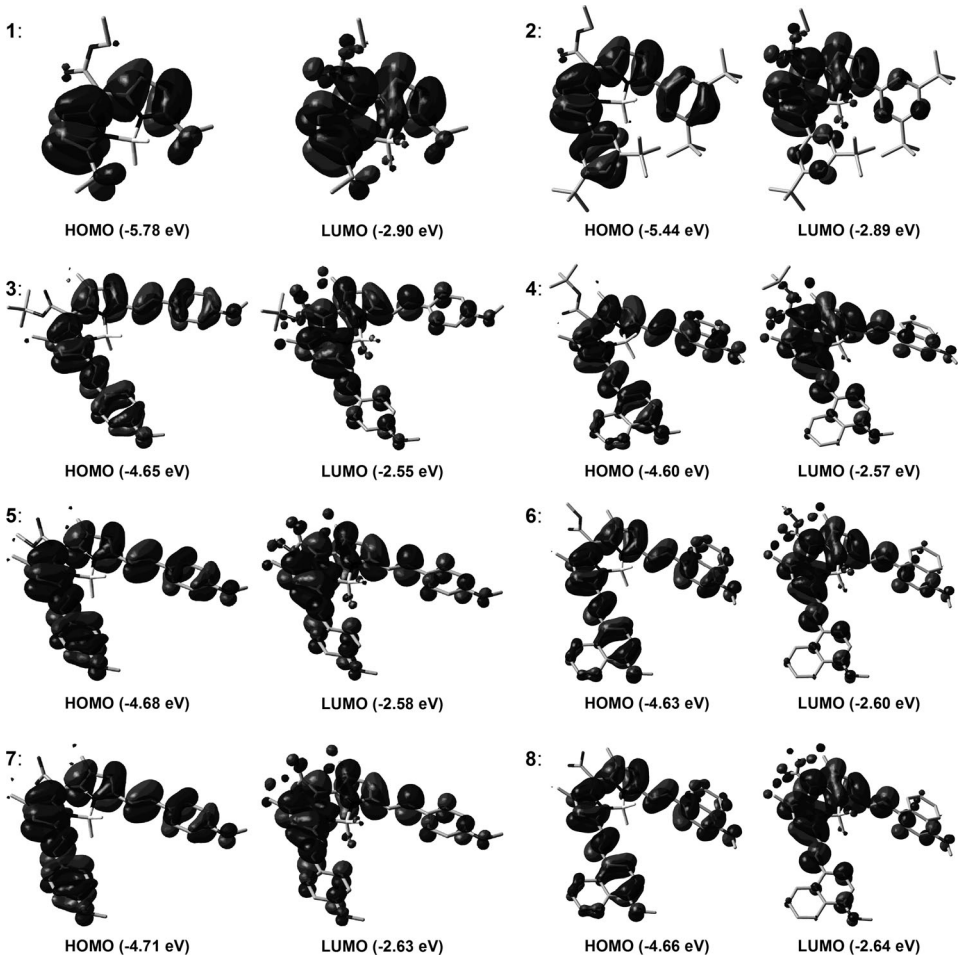

Figure 5. Calculated frontier molecular orbital profiles and the HOMO/LUMO energy levels of **1**–**8**. For simplification of the calculations, the ethylene glycol ether groups were replaced with methoxy groups.

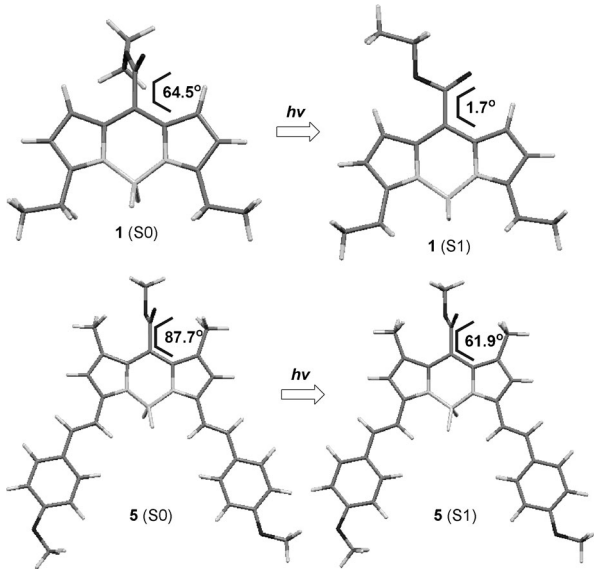

Figure 6. Calculated geometries of the ground states (S0) and first excited states (S1) of molecules **1** and **5**. For simplification of the calculations, the ethylene glycol ether groups in molecule **5** were replaced with methoxy groups.

methane and methanol, respectively.[25] UV/Vis/NIR absorption spectra were generated assuming an average UV/Vis width of 3000 cm^{-1} at half-height by using the SWizard program.[26]

The calculated frontier molecular orbital profiles and energy levels are shown in Figure 5. For dyes **2**–**8**, the HOMOs are delocalized through the BODIPY core to the aryl substituents, whereas the LUMOs are located mainly on the BODIPY core with a partial disjoint feature, indicating an intramolecular push–pull character, which also explains the large redshift in the absorption spectra. TD DFT calculations also predicted that dyes **1**–**8** would show absorption maxima at 423, 505, 596, 634, 592, 631, 594, and 634 nm (under vacuum), respectively, and this trend is consistent with the experimental data.

The much larger Stokes shifts observed for **1** and **2** in comparison with the other dyes (**3**–**8**) is also an interesting feature. For a further understanding of the origin of this difference, the ground state (S0) and the first excited singlet state (S1) of molecules **1** and **5** were calculated in CH_2Cl_2 and MeOH, respectively. The optimized geometry of **1** in the S0 state shows a large twist of the ester group from the BODIPY plane with a torsion angle of 64.5°, which becomes much smaller (1.7°) in the S1 state (Figure 6). Such a significant change in geometry from the S0 to S1 state should be ascribed to the large Stokes shift observed in **1**. On the other hand, the torsion angle of **5** changes from 87.7° in the S0 state to 61.9° in the S1 state, and such a small change in geometry can explain the relatively smaller Stokes shift observed for **5**. The two methyl groups at the β positions in molecules **3**–**8** are supposed to limit the free rotation of the ester or carboxylic acid group, thus leading to a small Stokes shift. The TD DFT calculations in solvents revealed that **1** in CH_2Cl_2 would show S0→S1 absorption and S1→S0 emission at 441 and 509 nm, respectively (Stokes shift = 3027 cm^{-1}), and **5** in MeOH would exhibit S0→S1 absorption and S1→S0 emission at 637 and 685 nm, respectively (Stokes shift = 1100 cm^{-1}). Such a trend is in reasonable agreement with the experimental data. Therefore, for future design, it would be essential to keep the two β sites of the BODIPY core unsubstituted if a larger Stokes shift were required.

Cell-staining tests

Encouraged by the outstanding features of the *meso*-ester- and *meso*-COOH-substituted BODIPYs, we next employed an epifluorescent microscope to examine the imaging ability of these dyes in living HeLa cells (Figure 7). Each dye (1 μM) was treated in live HeLa cell for 1 h and an image was then taken under a Cy5, Texas Red, or NIR filter according to the excitation and emission wavelength of the dye. The nucleus of the cell was stained with Hoechst, and an image was taken under a DAPI filter. The images were both taken with a 40× objective lens and merged.[27]

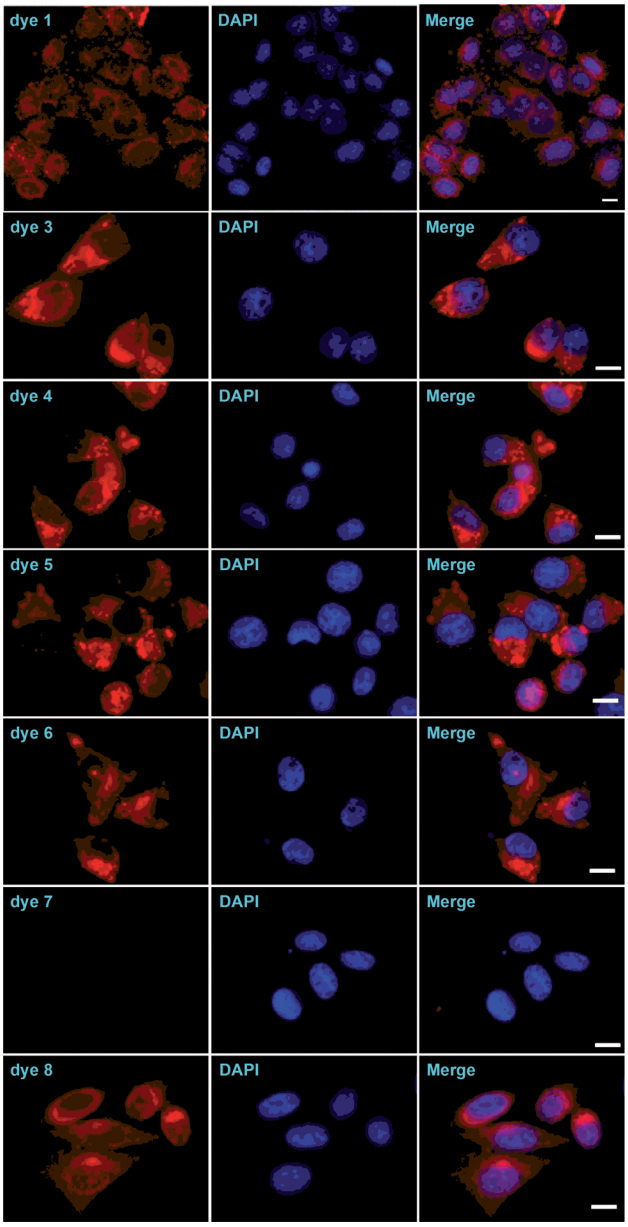

Figure 7. Living HeLa cell staining with dyes **1**–**8**. 1 μM of the dye was treated in live HeLa cells for 1 h and images were taken under a Texas Red filter (for **1**, **3**), NIR filter (for **4**, **6**), or Cy5 filter (for **5**, **7**, **8**). Nuclei were stained using Hoechst, and images were taken under a DAPI filter. Scale bar: 10 μm.

HeLa cells loaded with **1** showed a bright red cell profile. Strong fluorescence from the cellular cytoplasm was observed for dye-loaded HeLa cells, implying that dye **1** can diffuse efficiently into HeLa cells and be retained within them, thus confirming its membrane permeability. However, dye **2** was not appropriate for cell-imaging experiments owing to its high hydrophobicity, and thus, low solubility in cell growth media.

For the BODIPY dyes functionalized at the α positions (**3**–**8**), the extended π conjugation induced a significant redshift in absorption and emission, whereas the coupled oligo(ethylene glycol) ether groups would improve the hydrophilicity by forming a hydrophilic terminal within the structure. It was found that all the *meso*-ester-substituted BODIPYs **3**–**6** could stain HeLa cells successfully. For **3**, the Texas Red filter was used because the emission wavelength is within the far-red region. A deep red cell profile was observed, and the merged picture indicated that this dye was localized mainly in the cytoplasm, similarly to dye **1**. The NIR filter was employed for the image of the HeLa cell stained with **4** because of its emission at 727 nm (NIR region); a deep red cell profile was also observed, with the dyes staining mainly in the cytoplasm. The cell-staining tests of dyes **5** and **6** showed similar results (the Cy5 filter was used for **5**). The cell-imaging results indicate that all four functionalized *meso*-ester dyes are very cell-membrane-permeable, which allowed them to diffuse into the HeLa cells and be retained within them. The cell profiles of deep red color were observed through epifluorescent microscopy, implying that far-red or even NIR imaging can be realized by using these *meso*-ester-substituted BODIPYs. Cell-staining tests were also conducted for the two water-soluble dyes **7** and **8**. The experimental results indicated that **7** cannot penetrate and stain HeLa cells even if the concentration is raised to 9 μM. The membrane impermeability of compound **7** may be attributed to its high polarity and the hindrance from the membrane and the negatively charged cell components, which would block its penetration into the cell. However, when live HeLa cells were treated with **8** (1 μM) for 1 h and an image was taken under the Cy5 filter, a deep red stained cell profile was displayed, implying that **8** can diffuse efficiently into HeLa cells and remain within them.

Overall, the balance between the hydrophobicity and hydrophilicity of the new dyes can be adjusted for biological staining purposes through modification at the *meso* and α positions. Furthermore, it is reasonable to expect that after binding with some specific probes or drug molecules at the *meso*-COOH site, the resulting conjugated compounds would tend to be cell-membrane-permeable, opening the path for targetted bioimaging.

Conclusion

In summary, the *meso*-COOEt-substituted BODIPY derivatives **1** and **2** were first synthesized and characterized. Motivated by its bright fluorescence with large Stokes shift, we modified the structure further and prepared four *meso*-ester-substituted BODIPYs with extended π conjugation (**3**–**6**). After the introduction of oligo(ethylene glycol)-ether-substituted phenylene

vinylene or naphthalene vinylene groups, the absorption and emission maxima shifted to the far-red and NIR region. The resulting *meso*-ester-substituted BODIPY dyes also became partially water-soluble with appreciable fluorescence quantum yields. Moreover, cell-staining tests indicated that they sufficiently membrane-permeable to penetrate into living HeLa cells. All these features make these dyes attractive for bioimaging applications. Three different synthetic approaches to access the *meso*-COOH-substituted BODIPYs **7** and **8** were attempted, two of which were feasible, and one of which was a three-step, highly efficient, convenient synthetic route. The *meso*-COOH-substituted BODIPYs **7** and **8** were soluble in pure water and displayed remarkable fluorescence quantum yields at wavelengths around or above 650 nm. The carboxylic group can act as a versatile binding site to connect some specific probes for biotargeting and sensing applications. In addition, our synthetic strategies can be adapted easily for the preparation of a series of *meso*-COOH-substituted push–pull-type BODIPY dyes, which have good potential for applications in dye-sensitized solar cells.[18] The related studies are underway in our laboratory.

Experimental Section

General procedures

All reagents were purchased from commercial suppliers, and were used as received without further purification. Anhydrous dichloromethane and DMF were distilled from CaH_2. Toluene and THF were distilled from sodium benzophenone immediately prior to use. The ^{1}H NMR and ^{13}C NMR spectra were recorded on a Bruker DPX 300 or DRX 500 NMR spectrometer with tetramethylsilane as the internal standard. The chemical shift was recorded in ppm, and the following abbreviations are used for the multiplicities: s = singlet, d = doublet, t = triplet, q = quartet, m = multiplet. EI mass spectra were recorded on an Agilent 5975C DIP/MS mass spectrometer. MALDI-TOF-mass measurements were taken on a Bruker Autoflex instrument with anthracence-1,8,9-triol as the matrix. UV/Vis spectra and fluorescence spectra were recorded on a Shimadzu UV-1700 spectrometer and RF-5301 fluorometer, respectively. The solvents used for UV/Vis and PL measurements were of HPLC grade. Cell-staining images were taken under confocal microscopy upon living HeLa cells; the nuclei were stained with Hoechst and images were recorded under a DAPI filter. Images were taken with a 40× objective lens and merged.

Syntheses

Compound 1: Dry DCM (30 mL) in a round-bottomed flask was purged with nitrogen for 10 min. To this solution, ethyl glyoxalate (50% in toluene, 204 mg, 1 mmol), 2-ethyl pyrrole (234 mg, 2.2 mmol), and two drops of TFA were added. The reaction mixture was stirred for 3 h at RT. After complete consumption of the aldehyde (monitored by TLC), DDQ (248 mg, 1.1 mmol) was added to the reaction mixture. After 60 min, triethylamine (4 mL) and $BF_3{\cdot}OEt_2$ (5 mL) were added to the mixture. The resulting mixture was stirred at room temperature for 1 h. When the reaction was complete, the solvent was removed under reduced pressure. The residue was purified by column chromatography (silica gel, EtOAc/hexane, 1:3, v/v) to give **1** as a red solid (64 mg, 20%). ^{1}H NMR (500 MHz, $CDCl_3$): $\delta = 7.26$ (d, $J = 3.2$ Hz, 2H), 6.39 (d, $J = 3.2$ Hz, 2H), 4.47 (q, $J = 6.9$ Hz, 2H), 3.04 (q, $J = 7.6$ Hz, 4H), 1.44 (m, 3H), 1.34 ppm (m, 6H); ^{13}C NMR (125 MHz, $CDCl_3$): $\delta = 166.4$, 163.9, 133.1, 130.7, 128.9, 118.5, 62.5, 29.7, 22.3, 14.2, 12.6 ppm; HRMS (EI): *m/z* calcd for $C_{16}H_{19}BO_2F_2N_2$: 320.1510; found: 320.1508 ($[M]^+$).

Compound 2: Dry DCM (50 mL) in a round-bottomed flask was purged with nitrogen for 15 min. To this solution, ethyl glyoxalate (50% in toluene, 204 mg, 1 mmol), 2-(3,5-di-*tert*-butylphenyl) pyrrole[10a] (561 mg, 2.2 mmol), and TFA (two drops) were added. The reaction mixture was stirred for 3 h at room temperature. After complete consumption of the aldehyde (monitored by TLC), DDQ (248 mg, 1.1 mmol) was added to the reaction mixture. After 30 min, triethylamine (4 mL) and $BF_3{\cdot}OEt_2$ (5 mL) were added to the mixture. The resulting mixture was stirred at room temperature for 1 h. When the reaction was complete, the solvent was removed under reduced pressure. The residue was purified by column chromatography (silica gel, EtOAc/hexane, 1:5, v/v) to give **2** as a blue solid (179 mg, 28%). ^{1}H NMR (500 MHz, $CDCl_3$): $\delta = 7.69$ (d, $J = 1.9$ Hz, 4H), 7.47 (d, $J = 1.9$ Hz, 2H), 7.37 (d, $J = 3.8$ Hz, 2H), 6.64 (d, $J = 3.8$ Hz, 2H), 4.53 (q, $J = 7.6$ Hz, 2H), 1.49 (t, $J = 7.6$ Hz, 3H), 1.33 ppm (s, 36H); ^{13}C NMR (125 MHz, $CDCl_3$): $\delta = 164.1$, 162.0, 150.4, 134.9, 131.8, 130.3, 129.5, 124.3, 123.7, 122.1, 62.6, 34.9, 31.4 ppm; HRMS (EI): *m/z* calcd for $C_{40}H_{51}BO_2F_2N_2$: 640.4012; found: 640.3999 ($[M]^+$).

Compound 15: Benzyl alcohol (10.8 g, 100 mmol) in dry DCM (20 mL) was added through a syringe pump to a solution of oxalyl chloride (12.7 g, 100 mmol) in anhydrous DCM (50 mL) over 0.5 h. The solvent was removed in vacuo, affording benzyl chlorooxalate **14** as a colorless oil. Compound **14** was then used directly for the next step of the reaction without further purification. The solution of previously generated colorless oil (2 g, 10.1 mmol) in anhydrous DCM (20 mL) was added dropwise to the solution of 2,4-dimethylpyrrole (2.4 g, 25.4 mmol) in dry DCM (50 mL) through a syringe pump over 1 h at −78 °C under an Ar atmosphere. The resulting mixture was stirred at this temperature for 4 h, after which Et_3N (5.6 mL, 40.4 mmol) was added slowly, and the color of the solution turned to red–brown. Subsequently, $BF_3{\cdot}OEt_2$ (8.0 mL, excess) was added, and the solution was warmed slowly to room temperature and stirred for a further 2 h. After removal of the solvent under reduced pressure, the residue was purified by column chromatography (silica gel, DCM/hexane = 1:6 to 1:2) to afford compound **15** as a dark red solid (1.76 g, 45%). ^{1}H NMR ($CDCl_3$ 500 MHz): $\delta = 7.38$–7.43 (m, 5H), 6.03 (s, 2H), 5.38 (s, 2H), 2.52 (s, 6H), 2.02 ppm (s, 6H); ^{13}C NMR ($CDCl_3$ 125 MHz): $\delta = 165.0$, 157.6, 141.2, 133.6, 129.2, 129.1, 128.8, 121.2, 68.6, 14.7, 12.7 ppm; HRMS (EI): *m/z* calcd for $C_{21}H_{21}BF_2N_2O_2$: 382.1664; found: 382.1656 ($[M]^+$).

Compound 22: Compound **22** was synthesized in 56% yield according to the same procedure as for compound **15** but with methyl chorooxalate. ^{1}H NMR ($CDCl_3$, 500 MHz): $\delta = 6.06$ (s, 2H0, 3.97 (s, 3H), 2.53 (s, 6H), 2.11 ppm (s, 6H); ^{13}C NMR ($CDCl_3$, 125 MHz): $\delta = 166.4$, 158.3, 141.7, 129.5, 129.4, 121.9, 53.8, 15.4, 13.2 ppm; HRMS (EI): *m/z* calcd for $C_{15}H_{17}BF_2N_2O_2$: 306.1351; found: 306.1337 ($[M]^+$).

Compound 20: Compound **20** synthesized by using the same procedure as for **15** and **22** resulted in a yield of only 4.7%. The procedure using compound **15** to generate compound **20** is described below. Compound **15** (500 mg, 1.31 mmol) was dissolved in DCM (10 mL), and a small amount of 10% Pd/C powder (5 mol%) was added under an Ar atmosphere. This was followed by the addition of MeOH (20 mL). The mixture was degassed and then filled with H_2 gas by using a balloon. The resulting mixture was then stirred at RT under a H_2 atmosphere (1 atm) for 5 h until no starting material remained. Pd/C was removed through filtration, and the solvent was evaporated under vacuum to afford the crude com-

pound **19** as a brown–red solid in almost quantitative yield. Without further purification, compound **19** was redissolved in a mixed solvent of *tert*-butanol (5 mL) and anhydrous diethyl ether (15 mL), and then, an excess amount of DCC was added fractionally in 5 h. The insoluble white solid was removed by filtration, the solvent was removed under rotary evaporation, and the residue was purified by column chromatography (silica gel, DCM) to afford compound **20** as a bright red solid (1.76 g, 45%). ^{1}H NMR ($CDCl_3$, 500 MHz): $\delta = 6.05$ (s, 2H), 2.53 (s, 6H), 2.26 (s, 6H), 1.64 ppm (s, 9H); ^{13}C NMR ($CDCl_3$, 125 MHz): $\delta = 166.1$, 158.1, 141.5, 129.3, 129.1, 121.7, 53.5, 28.2, 15.2, 13.0 ppm; MS (MALDI-TOF): *m/z* calcd for $C_{18}H_{23}BF_2N_2O_2$: 348.1821; found: 348.1803 ($[M]^+$).

General procedure for the Knoevenagel condensation

In a round-bottomed flask equipped with a Dean–Stark apparatus, the corresponding aldehyde (2.2 equiv), piperidine (2 mL), and AcOH (2 mL) were added to a solution of BODIPY (1 mmol) in toluene (20 mL). The solution was heated at reflux for 12 h. The mixture was cooled to room temperature and washed three times with water. The organic phase was dried over $MgSO_4$ and the solvent was evaporated under reduced pressure. The residue was purified by silica gel column chromatography to afford the desired compounds **17**, **3**, **4**, **5**, and **6**.

Compound 17: Yield: 47%; ^{1}H NMR ($CDCl_3$, 500 MHz): $\delta = 6.96$–7.55 (m, 37H), 6.66 (s, 2H), 5.40 (s, 2H), 2.08 ppm (s, 6H); ^{13}C NMR ($CDCl_3$, 125 MHz): $\delta = 166.3$, 154.7, 149.6, 147.8, 139.9, 137.3, 134.5, 130.8, 130.1, 129.8, 129.7, 129.5, 129.4, 125.8, 124.4, 122.9, 118.2, 117.8, 69.1, 13.6 ppm; MS (MALDI-TOF): *m/z* calcd for $C_{59}H_{47}BF_2N_4O_2$: 892.3760; found: 892.3717 ($[M]^+$).

Compound 3: Yield: 43%; ^{1}H NMR ($CDCl_3$, 500 MHz): $\delta = 7.57$ (m, 6H), 7.23 (d, $J = 4.8$ Hz, 2H), 6.94 (d, $J = 2.6$ Hz, 2H), 6.68 (s, 2H), 4.18 (t, 4H), 3.88 (t, 4H), 3.76 (m, 12H), 3.56 (t, 4H), 3.39 (s, 6H), 2.32 (s, 6H), 1.66 ppm (s, 9H); ^{13}C NMR ($CDCl_3$, 125 MHz): $\delta = 164.6$, 159.8, 153.9, 139.9, 136.6, 131.0, 129.6, 129.2, 127.7, 117.4, 117.2, 115.0, 72.0, 70.9, 70.7, 70.6, 69.7, 67.6, 59.0, 29.7, 28.5, 14.4 ppm; MS (MALDI-TOF): *m/z* calcd for $C_{46}H_{59}BF_2N_2O_{10}$: 848.4231; found: 848.4210 ($[M]^+$).

Compound 4: Yield: 39%; ^{1}H NMR ($CDCl_3$, 500 MHz): $\delta = 8.35$ (d, $J = 4.25$ Hz, 2H), 8.17 (d, $J = 4.25$ Hz, 2H), 8.06 (d, $J = 8.0$ Hz, 2H), 7.95 (d, $J = 4.0$ Hz, 2H), 7.73 (d, $J = 8$ Hz, 2H), 7.49–7.60 (m, 4H), 6.90 (d, $J = 8.0$ Hz, 2H), 6.84 (s, 2H), 4.36 (t, 4H), 4.02 (t, 4H), 3.82 (t, 4H), 3.66–3.72 (m, 8H), 3.55 (t, 4H), 3.37 (s, 6H), 2.38 (s, 6H), 1.69 ppm (s, 9H); ^{13}C NMR ($CDCl_3$,125 MHz): $\delta = 164.6$, 155.9, 154.0, 140.0, 133.1, 132.3, 131.2, 127.7, 127.1, 126.2, 125.7, 125.6, 125.3, 122.9, 119.4, 117.7, 105.3, 85.5, 71.9, 71.0, 70.7, 70.6, 69.7, 68.0, 59.0, 28.5, 14.4 ppm; MS (MALDI-TOF): *m/z* calcd for $C_{54}H_{63}BF_2N_2O_{10}$: 948.4544; found: 948.4521 ($[M]^+$).

Compound 5: Yield: 51%; ^{1}H NMR ($CDCl_3$, 500 MHz): $\delta = 7.60$ (m, 6H), 7.29 (m, 2H), 7.00 (d, $J = 4.35$ Hz, 4H), 6.74 (s, 2H), 4.23 (m, 4H), 4.0 (s, 3H), 3.94 (m, 4H), 3.70–3.80 (m, 12H), 3.62 (m, 4H), 3.45 (s, 6H), 2.22 ppm (s, 6H); ^{13}C NMR ($CDCl_3$, 125 MHz): $\delta = 166.1$, 159.9, 154.1, 139.3, 136.9, 130.8, 129.4, 129.2, 129.0, 117.5, 117.0, 115.0, 71.9, 70.8, 70.6, 70.5, 69.6, 67.5, 59.0, 52.9, 12.7 ppm; HRMS (ESI): *m/z* calcd for $C_{43}H_{53}BF_2N_2NaO_{10}$: 829.3661; found: 829.3685 ($[M+Na]^+$).

Compound 6: Yield: 48%; ^{1}H NMR ($CDCl_3$, 300 MHz): $\delta = 8.30$ (d, $J = 3.75$ Hz, 2H), 8.12 (d, $J = 4.05$ Hz, 2H), 8.02 (d, $J = 7.95$ Hz, 2H), 7.90 (d, $J = 4.2$ Hz, 2H), 7.66 (d, $J = 8.1$ Hz, 2H), 7.43–7.56 (m, 4H), 6.85 (d, $J = 4.05$ Hz, 2H), 6.79 (s, 2H), 4.32 (m, 4H), 3.95 (m, 7H), 3.77 (m, 4H), 3.63 (m, 8H), 3.50 (m, 4H), 3.33 (s, 6H), 2.17 ppm (s, 6H); ^{13}C NMR ($CDCl_3$, 75 MHz): $\delta = 166.2$, 156.0, 154.3, 139.5, 139.4, 133.4, 132.3, 131.0, 127.1, 126.1, 125.73, 125.70, 125.3, 125.0, 122.8, 119.2, 117.8, 105.3, 71.9, 71.0, 70.7, 70.6, 69.7, 68.0, 59.0, 53.0, 12.8 ppm; HRMS (ESI): *m/z* calcd for $C_{51}H_{57}BF_2N_2NaO_{10}$: 929.3975; found: 929.3973 ($[M+Na]^+$).

Synthesis of *meso*-COOH-substituted BODIPYs

Method 1: Concentrated HCl (1.0 mL) was added to a solution of *meso*-COO-*t*Bu-substituted BODIPY **3** or **4** (0.05 mmol) in CH_3NO_2. The mixture was then stirred in an ice-water bath for 4 h, and diluted with DCM (50 mL). The solution was dried over Na_2SO_4, and the solvent was removed through rotary evaporation. The residue was purified by column chromatography (silica gel, DCM/MeOH = 10:1) to give the expected compound. Compound **7**, yield 28%; compound **8**, yield 22%.

Method 2: A mixture of *meso*-COOMe-substituted BODIPY **5** or **6** (0.10 mmol) and LiI (2.0 mmol) in dry ethyl acetate was heated to reflux for 16 h under an Ar atmosphere. The mixture was cooled to room temperature, and a small amount of HCl (0.2 mL) was added to quench the reaction. The organic layer was dried over Na_2SO_4 and the solvent was removed under vacuum. The residue was purified by column chromatography (silica gel, DCM/MeOH = 10:1) to give the target compounds. Compound **7**, yield 57%; compound **8**, yield 48%.

Compound 7: ^{1}H NMR (CD_3OD, 500 MHz): $\delta = 7.77$ (d, $J = 8.25$ Hz, 2H), 7.61 (d, $J = 4.5$ Hz, 4H), 7.27 (d, $J = 8.25$ Hz, 2H), 6.95 (d, $J = 4.5$ Hz, 4H), 6.82 (s, 2H), 4.15 (t, 4H), 3.84 (t, $J = 5.0$ Hz, 4H), 3.69 (m, 8H), 3.53 (m, 4H), 3.33 (s, 6H), 2.41 ppm (s, 6H); ^{13}C NMR (CD_3OD, 75 MHz): $\delta = 160.8$, 153.9, 140.5, 135.7, 132.6; 131.5, 129.9, 118.9, 117.7, 117.5, 116.0, 115.9, 72.8, 71.6, 71.4, 71.2, 70.7, 68.7, 59.1, 13.3 ppm; HRMS (ESI): *m/z* calcd for $C_{42}H_{51}BF_2N_2NaO_{10}$:815.3503; found: 815.3534 ($[M+Na]^+$).

Compound 8: ^{1}H NMR (CD_3OD, 500 MHz): $\delta = 8.34$ (d, 4H), 8.14 (d, $J = 8.0$ Hz, 2H), 8.03 (d, $J = 4.25$ Hz, 2H), 7.98 (d, $J = 8.0$ Hz, 2H), 7.64 (t, $J = 4.13$ Hz, 2H), 7.53 (t, $J = 4.13$ Hz, 2H), 7.10 (s, 2H), 7.05 (d, $J = 4.25$ Hz, 2H), 4.41 (m, 4H), 4.05 (m, 4H), 3.81 (m, 4H), 3.71 (m, 4H), 3.65 (m, 4H), 3.53 (m, 4H), 3.36 (s, 6H), 2.47 ppm (s, 6H); ^{13}C NMR (CD_3OD, 125 MHz): 162.8, 155.5, 139.2, 132.3, 131.5, 126.9, 126.5, 125.6, 125.0, 124.9, 122.9, 122.3, 119.8, 116.94, 116.86, 105.1, 71.5, 70.5, 70.2, 70.0, 69.5, 68.0, 57.8, 11.9 ppm; HRMS (ESI): *m/z* calcd for $C_{50}H_{55}BF_2N_2NaO_{10}$: 891.3816; found: 891.3788 ($[M+Na]^+$) .

Acknowledgements

The work was supported financially by the A*STAR BMRC grant (10/1/21/19/642), the Singapore-Peking-Oxford Research Enterprise (SPORE) (COY-15-EWI-RCFSA/N197–1), MOE Tier 2 grant (MOE2011-T2–2–130), and IMRE core funding (IMRE/13–1C0205).

Keywords: bioimaging · BODIPY · dyes · fluorescent probes · membrane permeability · near-infrared

[1] a) J. Fabian, H. Nakanzumi, M. Matsuoka, *Chem. Rev.* **1992**, *92*, 1197; b) A. Loudet, K. Burgess, *Chem. Rev.* **2007**, *107*, 4891; c) R. Ziessel, G. Ulrich, A. Harriman, *New J. Chem.* **2007**, *31*, 496; d) G. Ulrich, R. Ziessel, A. Harriman, *Angew. Chem.* **2008**, *120*, 1202; *Angew. Chem. Int. Ed.* **2008**, *47*, 1184; e) G. Qian, Z. Wang, *Chem. Asian J.* **2010**, *5*, 1006; f) N. Boens, V. Leen, W. Dehaen, *Chem. Soc. Rev.* **2012**, *41*, 1130; g) K. D. Piatkevich, F. V. Subach, V. V. Verkhusha, *Chem. Soc. Rev.* **2013**, *42*, 3441; h) L. Yuan, W. Lin, K. Zheng, L. He, W. Huang, *Chem. Soc. Rev.* **2013**, *42*, 622.

[2] a) L. Lavis, R. T. Raines, *ACS Chem. Biol.* **2008**, *3*, 142; b) V. P. Boyarskiy, V. N. Belov, R. Medda, B. Hein, M. Bossi, S. W. Hell, *Chem. Eur. J.* **2008**, *14*, 1784; c) J. Jose, K. Burgess, *J. Org. Chem.* **2006**, *71*, 7835.

[3] a) R. P. Haughland, *Handbook of Fluorescent Probes and Research Chemicals*, 9th ed., Molecular Probes, Eugene, OR, **2002**; b) A. Mishra, R. K. Behera, P. K. Behera, B. K. Mishra, G. B. Behera, *Chem. Rev.* **2000**, *100*, 1973; c) A. Ajayaghosh, *Acc. Chem. Res.* **2005**, *38*, 449; d) J. J. McEwen, K. J. Wallace, *Chem. Commun.* **2009**, 6339.

[4] a) G. T. Hermanson, *Bioconjugate Techniques, 2nd ed.*, Thermo Fisher Scientific: Rockford, IL, **2008**; b) S. A. Farber, M. Pack, S. Y. Ho, I. D. Johnson, D. S. Wagner, R. Dosch, M. C. Mullins, H. S. Hendrickson, E. K. Hendrickson, M. E. Halpern, *Science* **2001**, *292*, 1385; c) J. M. Palomo, M. Lumbierres, H. Waldmann, *Angew. Chem.* **2006**, *118*, 491; *Angew. Chem. Int. Ed.* **2006**, *45*, 477; d) V. Ntziachristos, J. Ripoll, L. V. Wang, R. Weissleder, *Nat. Biotechnol.* **2005**, *23*, 313; e) J. Murtagh, D. O. Frimannsson, D. F. O'Shea, *Org. Lett.* **2009**, *11*, 5386; f) M. Tasior, D. F. O'Shea, *Bioconjugate Chem.* **2010**, *21*, 1130.

[5] Y. Urano, D. Asanuma, Y. Hama, Y. Koyama, T. Barrett, M. Kamiya, T. Nagano, T. Watanabe, A. Hasegawa, P. L. Choyke, H. Kobayashi, *Nat. Med.* **2009**, *15*, 104.

[6] T. Kowada, J. Kikuta, A. Kubo, M. Ishii, H. Maeda, S. Mizukami, K. Kikuchi, *J. Am. Chem. Soc.* **2011**, *133*, 17772.

[7] a) A. Burghart, H. Kim, M. B. Welch, L. H. Thoresen, J. Reibenspies, K. Burgess, F. Bergstrorm, L. B. A. Johansson, *J. Org. Chem.* **1999**, *64*, 7813; b) Y.-H. Yu, A. B. Descalzo, Z. Shen, H. Röhr, Q. Liu, Y.-W. Wang, M. Spieles, Y.-Z. Li, K. Rurack, X.-Z. You, *Chem. Asian J.* **2006**, *1*, 176; c) T. Rohand, M. Baruah, W. Qin, N. Boens, W. Dehaen, *Chem. Commun.* **2006**, 266; d) M. Baruah, W. Qin, R. A. L. VallQe, D. Beljonne, T. Rohand, W. Dehaen, N. Boens, *Org. Lett.* **2005**, *7*, 4377.

[8] a) J. Chen, J. Reibenspies, A. Derecskei-Kovacs, K. Burgess, *Chem. Commun.* **1999**, 2501; b) K. Umezawa, Y. Nakamura, H. Makino, D. Citterio, K. Suzuki, *J. Am. Chem. Soc.* **2008**, *130*, 1550; c) A. Matsui, K. Umezawa, Y. Shindo, T. Fujii, D. Citterio, K. Oka, K. Suzuki, *Chem. Commun.* **2011**, *47*, 10407; d) S. G. Awuah, J. Polreis, V. Biradar, Y. You, *Org. Lett.* **2011**, *13*, 3884; e) A. Wakamiya, T. Murakami, S. Yamaguchi, *Chem. Sci.* **2013**, *4*, 1002; f) Y. Ni, W. Zeng, K. Huang, J. Wu, *Chem. Commun.* **2013**, *49*, 1217.

[9] a) W. Zhao, E. M. Carreira, *Angew. Chem.* **2005**, *117*, 1705; *Angew. Chem. Int. Ed.* **2005**, *44*, 1677; b) W. Zhao, E. M. Carreira, *Chem. Eur. J.* **2006**, *12*, 7254; c) S. O. McDonnell, D. F. O'Shea, *Org. Lett.* **2006**, *8*, 3493.

[10] a) C. Jiao, K.-W. Huang, J. Wu, *Org. Lett.* **2011**, *13*, 632; b) C. Jiao, L. Zhu, J. Wu, *Chem. Eur. J.* **2011**, *17*, 6610; c) L. Zeng, C. Jiao, X. Huang, K.-W. Huang, W.-S. Chin, J. Wu, *Org. Lett.* **2011**, *13*, 6026; d) Y. Hayashi, N. Obata, S. Seki, Y. Kureishi, S. Saito, S. Yamaguchi, H. Shinokubo, *Org. Lett.* **2012**, *14*, 866; e) C. Jones, T. Suarez, *J. Org. Chem.* **1972**, *37*, 3622.

[11] a) M. Tera, K. Iida, K. Ikebukuro, H. Seimiya, K. Shin-yac, K. Nagasawa, *Org. Biomol. Chem.* **2010**, *8*, 2749; b) H. R. Davison, S. Taylor, C. Drake, P.-W. Phuan, N. Derichs, C. Yao, E. F. Jones, J. Sutcliffe, A. S. Verkman, M. J. Kurth, *Bioconjugate Chem.* **2011**, *22*, 2593; c) D. Das, Z. Tnimov, U. T. T. Nguyen, G. Thimmaiah, H. Lo, D. Abankwa, Y. Wu, R. S. Goody, H. Waldmann, K. Alexandrov, *ChemBioChem* **2012**, *13*, 674; d) Z. Zhang, P. Gao, X. Guo, H. Wang, H. Zhang, *Anal. Bioanal. Chem.* **2011**, *401*, 1905; e) S. Hoogendoorn, K. L. Habets, S. Passemard, J. Kuiper, G. A. van der Marel, B. I. Floreaa, H. S. Overkleeft, *Chem. Commun.* **2011**, *47*, 9363.

[12] a) S. Atilgan, T. Ozdemir, E. U. Akkaya, *Org. Lett.* **2008**, *10*, 4065; b) S. Zhu, J. Zhang, G. Vegesna, F. Luo, S. A. Green, H. Liu, *Org. Lett.* **2011**, *13*, 438; c) M. Isik, T. Ozdemir, I. S. Turan, S. Kolemen, E. U. Akkaya, *Org. Lett.* **2013**, *15*, 216; d) G. K. Vegesna, S. R. Sripathi, J. Zhang, S. Zhu, W. He, F. Luo, H. Liu, *ACS Appl. Mater. Interfaces* **2013**, *5*, 4107; e) T. Bura, P. Retailleau, G. Ulrich, R. Ziessel, *J. Org. Chem.* **2011**, *76*, 1109.

[13] a) D. Wang, J. Fan, X. Gao, B. Wang, S. Sun, X. Peng, *J. Org. Chem.* **2009**, *74*, 7675; b) F. Wang, X. Xiong, X. Guo, H. Wang, H. Zhang, *J. Chromatogr. A* **2013**, *1291*, 84 – 91.

[14] a) S. L. Niu, G. Ulrich, R. Ziessel, A. Kiss, P. Y. Renard, A. Romieu, *Org. Lett.* **2009**, *11*, 2049;b) L. Li, J. Han, B. Nguyen, K. Burgess, *J. Org. Chem.* **2008**, *73*, 1963.

[15] K. Krumova, G. Cosa, *J. Am. Chem. Soc.* **2010**, *132*, 17560.

[16] T. Komatsu, D. Oushiki, A. Takeda, M. Miyamura, T. Ueno, T. Terai, K. Hanaoka, Y. Urano, T. Mineno, T. Nagano, *Chem. Commun.* **2011**, *47*, 10055.

[17] R. M. Denton, J. An, B. Adeniran, A. J. Blake, W. Lewis, A. M. Poulton, *J. Org. Chem.* **2011**, *76*, 6749.

[18] a) T. Bura, N. Leclerc, S. Fall, R. Ziessel, *J. Am. Chem. Soc.* **2012**, *134*, 17404; b) S. Kolemen, O. A. Bozdemir, Y. Cakmak, G. Barin, S. Erten-Ela, M. Marszalek, J. Yum, S. M. Zakeeruddin, M. K. Nazeeruddin, E. U. Akkaya, *Chem. Sci.* **2011**, *2*, 949.

[19] E. C. Taylor, G. S. K. Wong, *J. Org. Chem.* **1989**, *54*, 3618.

[20] A. K. Chakraborti, M. K. Nayak, L. Sharma, *J. Org. Chem.* **2002**, *67*, 1776.

[21] J. W. Fisher, K. L. Trinkle, *Tetrahedron Lett.* **1994**, *35*, 2505.

[22] L. N. Sobenina, A. M. Vasil'tsov, O. V. Petrova, K. B. Petrushenko, I. A. Ushakov, G. Clavier, R. Meallet-Renault, A. I. Mikhaleva, B. A. Trofimov, *Org. Lett.* **2011**, *13*, 2524.

[23] Y. Chen, J. Zhao, H. Guo, L. Xie, *J. Org. Chem.* **2012**, *77*, 2192.

[24] a) A. D. Becke, *J. Chem. Phys.* **1993**, *98*, 5648; b) C. Lee, W. Yang, R. G. Parr, *Phys. Rev. B* **1988**, *37*, 785; c) R. W. Ditchfield, J. Hehre, J. A. Pople, *J. Chem. Phys.* **1971**, *54*, 724; d) W. J. Hehre, R. Ditchfield, J. A. Pople, *J. Chem. Phys.* **1972**, *56*, 2257; e) P. C. Hariharan, J. A. Pople, *Theor. Chim. Acta* **1973**, *28*, 213.

[25] J. Tomasi, B. Mennucci, R. Cammi, *Chem. Rev.* **2005**, *105*, 2999 – 3093.

[26] Gorelsky, S. I., *SWizard program*, http://www.sg-chem.net/, University of Ottawa, Ottawa, Canada, **2010**.

[27] J. Lee, N. Kang, Y. K. Kim, A. Samanta, S. Feng, H. K. Kim, M. Vendrell, J. H. Park, Y. Chang, *J. Am. Chem. Soc.* **2009**, *131*, 10077.

Received: October 3, 2013
Published online on January 21, 2014

